Hypertension Research (2018) 41:1013–1022
https://doi.org/10.1038/s41440-018-0105-6

ARTICLE

Upregulation of Nav1.6 expression in the rostral ventrolateral medulla of stress-induced hypertensive rats

Jia-Xiang Wu[1] · Lei Tong[1] · Li Hu[1] · Chun-Mei Xia[1,2] · Min Li[1] · Qing-Hui Chen[3] · Fu-Xue Chen[1] · Dong-Shu Du[1]

Received: 1 December 2017 / Revised: 6 April 2018 / Accepted: 9 April 2018 / Published online: 4 October 2018

Abstract

The rostral ventrolateral medulla (RVLM) plays a key role in mediating the development of stress-induced hypertension (SIH) by excitation and/or inhibition of sympathetic preganglionic neurons. The voltage-gated sodium channel Nav1.6 has been found to contribute to neuronal hyperexcitability. To examine the expression of Nav1.6 in the RVLM during SIH, a rat model was established by administering electric foot-shocks and noises. We found that Nav1.6 protein expression in the RVLM of SIH rats was higher than that of control rats, peaking at the tenth day of stress. Furthermore, we observed changes in blood pressure correlating with days of stress, with systolic blood pressure (SBP) found to reach a similarly timed peak at the tenth day of stress. Percentages of cells exhibiting colocalization of Nav1.6 with NeuN, a molecular marker of neurons, indicated a strong correlation between upregulation of Nav1.6 expression in NeuN-positive cells and SBP. The level of RSNA was significantly increased after 10 days of stress induction than control group. Compared with the SIHR, knockdown of Nav1.6 in RVLM of the SIHR decreased the level of SBP, heart rate (HR) and renal sympathetic nerve activity (RSNA). These results suggest that upregulated Nav1.6 expression within neurons in the RVLM of SIH rats may contribute to overactivation of the sympathetic system in response to SIH development.

Keywords: Stress · Hypertension · Nav1.6 · RVLM · Neuron

Introduction

Stress-induced hypertension (SIH), which results from central sympathetic nerve disorder, is the major aggravating cause of social and psychological stress among adults [1]. Stress can activate a series of pathological molecular and cellular alterations, leading to activation of sympathetic neurons. Interestingly, several lines of experimental evidence have indicated a key role for the sympathetic nervous system in stress-mediated cardiovascular disease [2]. For instance, neuronal activity and sympathetic overactivity in the rostral ventrolateral medulla (RVLM) are involved in the regulation of hypertension [3].

The RVLM is integral for vasomotion, and controls arterial pressure and activation of the basal sympathetic nerve [4]. Several studies have demonstrated that presympathetic neurons in the RVLM are responsible for generating sympathetic drive to the cardiovascular system, eventually regulating both cardiac output and vascular resistance [5]. Recently, some interesting studies have shown that neurons located in the RVLM, such as C1 adrenaline-synthesizing neurons, express phenylethanolamine-*N*-methyl transferase. Photostimulation of these animals increases sympathetic nerve activity and blood pressure [6].

Voltage-gated sodium channels (VGSCs) play key roles in controlling the excitability of neurons, as they are indispensable to the propagation and initiation of action potentials [7]. VGSCs, which are important cell membrane components of a variety of excitable cell types, comprising an α-subunit and one or more of four auxiliary β-subunits.

These authors contributed equally: Jia-Xiang Wu, Lei Tong, Li Hu

Electronic supplementary material The online version of this article (https://doi.org/10.1038/s41440-018-0105-6) contains supplementary material, which is available to authorized users.

✉ Dong-Shu Du
sdhzdds@163.com

[1] Shanghai Key Laboratory of Bio-Crops, College of Life Science, Shanghai University, Shanghai, China

[2] Department of Physiology and Pathophysiology, Shanghai Medical College of Fudan University, Shanghai, China

[3] Department of Kinesiology and Integrative Physiology, Michigan Technological University, Houghton, MI, USA

The α-subunit is a principal structural component that forms the ion-conducting pore responsible for activation and inactivation of channel gating, while the four auxiliary β-subunits modulate the gating kinetics of the α-subunit [8]. In mammals, the *Nax* gene encodes ten α-subunit family members, Nav1.1−Nav1.9 [9]. Nav1.6 is the vital VGSC subtype mediating continual Na^+ currents into cells. Moreover, resurgent Na^+ currents contribute to the generation and transmission of neurotransmitters such as glutamic acid, as well as high-frequency firing [10]. Nav1.6 facilitates increased neuronal hyperexcitability during the development of epileptogenesis [11]. However, expression patterns of Nav1.6 in SIH are unknown. Thus, the purpose of this study was to investigate the expression and distribution of Nav1.6 in a rat model of SIH.

Material and methods

Animals and experimental design

All animal procedures were approved by the Institutional Animal Care and Use Committee (Department of Laboratory Animal Science, Shanghai University) and carried out in full accordance with institutional animal care use protocols of Laboratory Animals of Shanghai University. Adult Sprague-Dawley rats (male, weight range: 250–300 g) were used in all experiments. Animals were housed with 12-h light/dark cycles and free access to food and water; room temperature was maintained between 23 and 24 °C. The stress-induced hypertensive rat (SIHR) model was established as previously described [12]. Briefly, 20 animals were randomly divided into two groups: normotensive (control) and SIHR ($n = 10$ per group). Animals in the SIHR group were placed in a cage (22 cm × 22 cm × 28 cm) with a grid floor and subjected to electric foot-shocks. Delivery of intermittent electric shocks (35–75 V, 0.5 ms in duration) through the grid floor every 2–30 s was randomly controlled by a computer. Noises (range: 88–98 dB) produced by a buzzer were given synchronously as a conditioned stimulus. The computer program was designed to provide two types of stimuli: noise plus electric foot-shock or noise only, both of which were delivered randomly. On day 5 when systolic blood pressure (SBP) and HR of stressed groups increased to a nearly stable level, the computer linked to the stressor apparatus was adjusted, gradually decreasing electric foot-shock times and prolonging the interval between shocks until only the noise stimuli remained. The control group underwent sham stress, i.e. they were put into the cage for the same period of time, but were not subjected to foot-shocks or noises. Rats were subjected to stress for 2 h twice daily for l5 consecutive days. Two hours after being subjected to stress, SBP and HR was consciously measured using the tail-cuff method. Measurements were repeated three times and the average value was taken as the SBP and HR.

Measurement of renal sympathetic nerve activity

We recorded renal sympathetic nerve activity (RSNA) in SIHR. Briefly, rats were anesthetized (urethane 800 mg/kg, alphachloralose 40 mg/kg, i.p.) and the left kidney was exposed to the retroperitoneum through the left incision. The sympathetic nerve was identified by running on or beside the renal arteries and isolated. Then it was placed on a pair of silver recording electrodes (Teflon 786500, A-M System). Subsequently, Kwik-Sil gel (World Precision Instruments) was used to cover the exposed nerves and the electrodes. Grass P55C preamplifier was used to amplify and filter (bandwidth: 100–3000 Hz) the RSNA signal which was monitored on an oscilloscope when the gel had hardened. The signal was rectified, integrated, sampled (1 kHz),and converted to a digital signal to be displayed on a computer by PowerLab system (AD Instruments, Australia). The maximum nerve activity occurred 1–2 min after the rat was overdosed for narcotic euthanasia. Background noise levels for sympathetic nerve activity were recorded 15–20 min after the rat was euthanized. Using the unit conversion of Powerlab Chart (AD Instruments) system, baseline nerve activity was taken as percent of Max after the noise level was subtracted [13].

Delivery of lentivirus in RVLM of SIHR

Lentiviral vectors have been applied for the delivery of CRISPR/Cas9 system in vivo. A sequence-specific guide RNA was designed to target the gene encoding Nav1.6 and cloned into the lentiCRISPR-eGFP plasmid to knockdown Nav1.6 [14]. We used the lentiviral vectors to deliver the CRISPR/Cas9 system into the neurons in the RVLM. The Nav1.6 gRNA lentivirus (Lv-CRISPR-eGFP-Scn8a-gRNA) and nontargeting lentivirus (Lv-CRISPR-eGFP) were produced and purified by Shanghai Hanbio (Shanghai, China). Sequences for gRNAs targeting Nav1.6 gene were as follows: gRNA: 5′-CAAAGGCGGATGGCAGCCAC-3′. In this study, the rats were assigned to four groups ($n = 6$ per group): control, stress, stress with GFP (Lv-CRISPR-eGFP) and stress with gRNA (Lv-CRISPR-eGFP-Scn8a-gRNA). Lentiviral vector (2.1×10^6 TU) was microinjected into the RVLM of SIHR on the fifth day of stress.

RNA isolation and quantitative real-time RT-PCR

Total RNA from the RVLM was extracted with Total RNA extraction reagent (TaKaRa, Dalian, China). cDNA was synthesized using High Capacity cDNA Reverse

Transcription Kit (Applied Biosystems, ABI). Quantitative real-time PCR was performed using Brilliant SYBR Green QPCR Master Mix (TaKaRa, Japan). The specific primer sequences for Nav1.6 were forward 5′-AGGATGTTAGCA GCGAATCAGACC-3′ and reverse 5′-GGAGCTGGTATC GTCCAGTTTATC-3′. The primers for reference gene were as follows: beta-actin forward 5′-CGCGAGTACAACC TTCTTGCAG-3′ and reverse 5′-TATCGTCATCCATGGC GAACTGG-3′. Amplification and melting curves were recorded using an ABI 7500 system (Bio-Rad, USA).

Western blot analysis

Total membrane protein extracted from RVLM homogenates with a ProteinExtTM Mammalian Membrane Protein Extraction Kit (TransGenBiotech, Beijing, China) was used to analyze protein expression by western blot. Briefly, proteins from RVLM were separated by 6% SDS-PAGE and transferred onto PVDF membranes (0.45 μm; Millipore, Billerica, USA). Membranes were placed in QuickBlock Blocking Buffer for western blot (Beyotime, Beijing, China) for 30 min to block nonspecific binding sites before incubating overnight at 4 °C with primary antibody solution, and then 1 h at room temperature with secondary antibody solution. The primary antiserum used for western blot analysis included rabbit polyclonal antiserum to Nav1.6 (1:200; Abcam, Cambridge, UK), mouse polyclonal antiserum to GAPDH (1:1000; TransGenBiotech, Beijing China), goat anti-rabbit IgG-HRP (1:10,000; Santa Cruz Biotech, Santa Cruz, CA), and goat anti-mouse IgG-HRP (1:10,000; Santa Cruz Biotech). Fluorescent signals were detected using ECL detection reagents (WBKLS0050; Millipore) with a fully automatic chemiluminescence image analysis system (Tanon-5200; Tanon Science & Technology, Shanghai, China).

Immunofluorescence

Rats were anesthetized with chloral hydrate and perfused through the ascending aorta with 200 ml of heparinized saline followed by 200 ml of freshly prepared 4% paraformaldehyde in 0.1 M phosphate-buffered saline (PBS, pH 7.4). Brain tissues were removed and post-fixed in the same fixative for 12 h, then brain tissues were placed in 20% sucrose at 4 °C until they sunk to the bottom. After that, brain tissues were placed in 30% sucrose at 4 °C until they sunk to the bottom. Frozen 20-μm coronal sections were cut using a cryostat (Microm, Germany). First, sections were incubated in 0.2 mg/ml pepsin (Biotech Well) at 37 °C for 10–15 min according to the procedure developed by Lorincz [15], and then washed three times with 0.01 M PBS for 5 min. Sections were incubated for 30 min with 5% goat serum in 0.01 M PBS to block nonspecific binding sites, and then sections were incubated with primary antibodies overnight at 4 °C. The following day, sections were rinsed with 0.01 M PBS and incubated for 2 h with secondary antibodies at room temperature. Finally, coverslips were applied after sections were rinsed. The primary antiserum used for immunofluorescence analysis included rabbit polyclonal antiserum to Nav1.6 (1:300; Abcam), mouse polyclonal antiserum to NeuN (1:400; Abcam), goat polyclonal antiserum to Iba1 (1:400; Abcam), mouse polyclonal antiserum to GFAP (1:500; Abcam), donkey anti-rabbit IgG H&L Alexa Fluor 555 (1:500; Abcam), donkey anti-goat IgG H&L Alexa Fluor 488 (1:500; Abcam), and donkey anti-mouse IgG H&L Alexa Fluor 594 (1:500; Abcam).

Tissue analysis

Confocal images were obtained using a laser scan confocal fluorescence microscope (LSM710; Carl Zeiss, Jena, Germany) and saved as 16-bit TIFF files. Images from identical regions and layers of RVLM in control and SIHR (5, 10, and 15 days of stress) rats ($n = 4$–6 per group) were processed. Images were integrated and processed to enhance contrast using Nikon software (NS-Elements BR 4.2.00) with identical settings for different conditions. For quantification of Nav1.6-immunoreactive (Nav1.6-ir) cells and colocalization ratios between Nav1.6 and other cell markers in the RVLM, sections including the RVLM were assigned to levels from −12.00 to −12.48 mm from bregma according to Paxinos [16]. The number of animals in each group is the same. Colocalization ratios between Nav1.6 and other proteins including NeuN, GFAP, and Iba1 in six continuous RVLM sections were analyzed using Image-Pro Plus software 6.0. Numbers of Nav1.6-ir cells were counted in a 300 μm × 300 μm grid laid over the GCC in six continuous sections using Image-Pro Plus software 6.0 [17]. All data were collected by an investigator blinded to the treatment of each group.

Statistical analysis

SPSS 22.0 was used for statistical analyses. Statistical significance was assessed using one-way ANOVA followed by a post hoc Least Significant Difference test. Correlations were analyzed using Spearman's correlation test. All values are expressed as mean ± standard error of the mean, with a level of 0.05 as a threshold for statistical significance.

Results

Effects of chronic stress on SBP and HR

Rats were stimulated for 2 h daily for 15 consecutive days. Tail SBP and HR were measured in conscious rats after

daily stress. Obvious behavioral and physiological changes occurred in the SIHR group after the first 3–5 days of daily stress induction. Compared with the control group, the SIHR group exhibited increased anxiety in performance tests and significantly increased SBP and HR (Fig. 1a, c); however, animals in the SIHR group weighed less (Fig. 1b). Thus, it appears that stress has a significant effect on blood pressure, HR, and weight of rats. On the tenth day, SBP exhibited its peak increase after stress (from 100 ± 5 mmHg to 155 ± 8 mmHg; Fig. 1a), which was maintained over the next few days of stress induction. Thus, the tenth day was a very important day. It is noteworthy that the weight of rats in the SIHR group was significantly lower than that in the control group. Surprisingly, the weight of rats in the SIHR group was increased after the 12th day of stress compared with the control group (Fig. 1b). The SIHR group experienced a significant increase in SBP, HR and slowed growth for 15 consecutive days. These data supported the reliability and accuracy of our SIHR model.

Dynamic expression of Nav1.6 in the RVLM of SIHR

Western blotting was performed to investigate Nav1.6 expression at protein level in SIHR and control group. Nav1.6 protein levels were altered at numerous time points including 5, 10, and 15 days after stress induction. A significant difference in Nav1.6 expression in the RVLM was observed between the SIHR and control group. Expression of Nav1.6 protein was significantly higher in the SIHR group on the 10th and 15th days compared with the control group (Fig. 2a, b), with Nav1.6 protein levels within the RVLM peaking on the tenth day of stress (Fig. 2b). One possible explanation for this phenomenon is that the development of SIH results from the activation of Nav1.6 in the RVLM.

Immunofluorescence experiments were used to reveal the distribution and expression of Nav1.6 in the RVLM of SIHR and control group. Numbers of Nav1.6-immunoreactive (ir) cells in the RVLM of the SIHR group on the tenth day of stress was significantly higher than observed for control group rats (Fig. 2c, d). A previous study revealed that Nav1.6 immunoreactivity was located within the axonal initial segment and nodes of Ranvier, but was very sparse in the CPU and the cortex [18]. Interestingly, we observed the similar results that Nav1.6 immumoreactivity (ir) is sparse in the RVLM of control group rats, while in great amount in the SIHR group.

Colocalization of increased Nav1.6 with NeuN in the RVLM of SIHR

Double-immunofluorescence staining was used to ascertain the type of neural cells in which Nav1.6 is localized. NeuN is a prototypical marker for immunohistochemical identification of neurons, while GFAP is a specific protein marker of astrocytes, and Iba1 is considered to be a prototypical marker of microglia. The RVLM is located at 1.2 mm lateral to the midline, 5.3 mm ventral to the dorsal surface of the brain, and 1.9 mm caudal to lambda (Fig. 3a). In the SIHR group, a large number of NeuN and Nav1.6 double-positive cells were observed in the whole oblongata (Fig. 3b), and expression of Nav1.6-positive neurons in the RVLM was significantly increased compared with the control group (Fig. 3c).

Double-immunostaining demonstrated a steady increase in the number of Nav1.6 and NeuN double-positive cells as

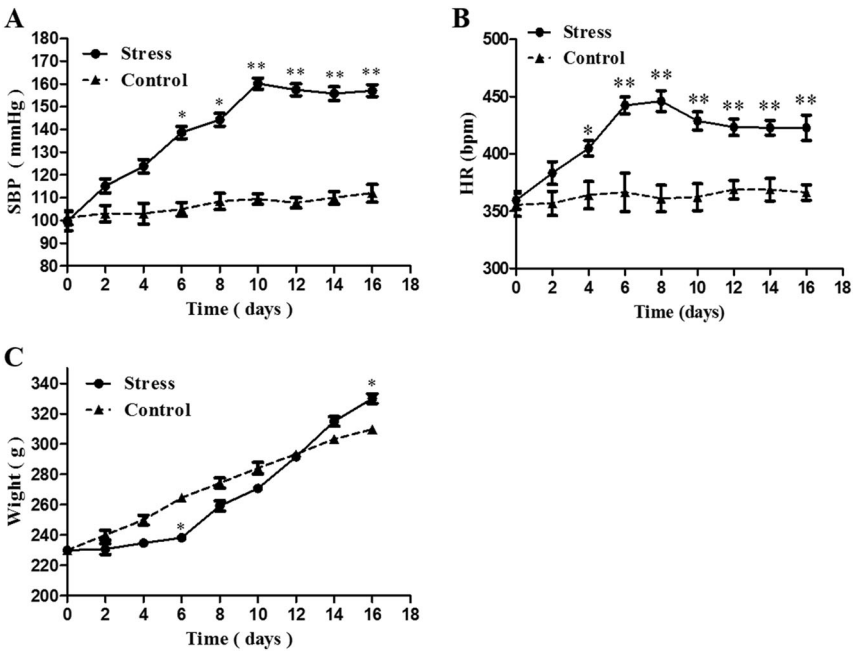

Fig. 1 Changes of systolic blood pressure (SBP), heart rate (HR), and weight between normotensive (control) and stress-induced hypertensive rat (SIHR) group during the observation period (0–15 days). Compared with the control group, the SIHR group exhibited increased anxiety in performance tests and significantly increased SBP and HR (Fig. 1a, c); however, animals in the SIHR group weighed less (Fig. 1b). $^{*}P < 0.05$, $^{**}P < 0.01$ vs. control group. Values represent mean ± standard error, n = 8.

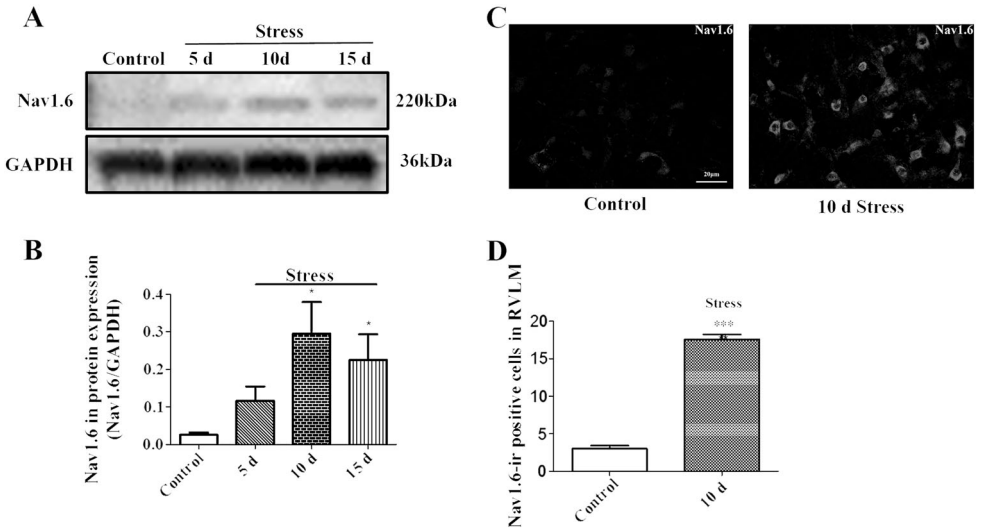

Fig. 2 Western blot analysis of Nav1.6 expression in the rostral ventrolateral medulla (RVLM) of normotensive (control) and stress-induced hypertensive rat (SIHR) group at different time points after stress. **a**, **b** Optical band density analysis revealed that Nav1.6 protein levels increased significantly at the 10th and 15th day after stress, and reached a peak at the tenth day. Bars represent mean ± standard error. $^{*}P < 0.05$, vs. control group, $n = 3$. **c**, **d** Statistical analysis of the number of Nav1.6-ir cells in the RVLM of control and SIHR group at the tenth day of stress showed a significant increase in the number of Nav1.6-ir cells in the RVLM of the SIHR group on the tenth day of stress compared with the control group. Bars represent mean ± standard error. $^{***}P < 0.001$, vs. control group, $n = 4$

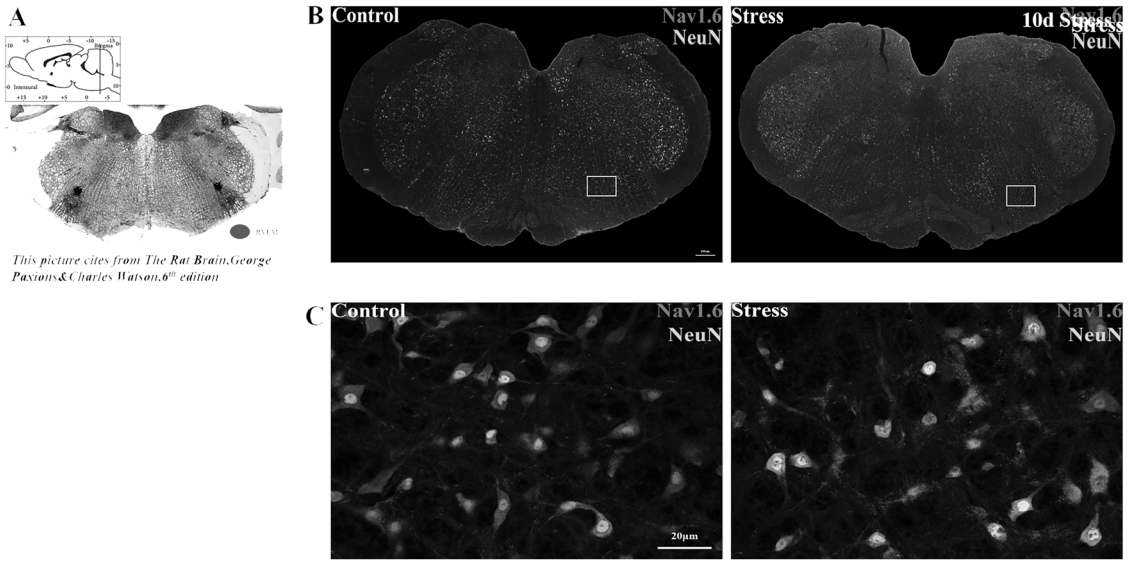

Fig. 3 Colocalization of Nav1.6 (red) with NeuN (green) in the rostral ventrolateral medulla (RVLM) of stress-induced hypertensive rat (SIHR) and normotensive (control) group. **a**, **b** Representative photomicrograph of the whole medulla oblongata in control and SIHR group at the tenth day of stress. **c** Colabeling of Nav1.6 and NeuN is indicated by yellow

days of stress increased, reaching a peak at the tenth day (Fig. 4a, b). We found that the number of NeuN-positive soma exhibiting colocalization with Nav1.6 decreased with increasing days of stress (Fig. 4a). Interestingly, in the RVLM, increased colocalization of Nav1.6 with NeuN and increased protein expression of Nav1.6 both positively correlated with increased days of stress and changes in SPB. In addition, we double-immunolabeled Nav1.6 with GFAP and Iba1 in the RVLM of rats, and induced stress in these animals for 10 days. Activation of microglia and astrocytes was not observed in the RVLM at the tenth day (Fig. 5).

Changes of SBP and RSNA by microinjection of Nav 1.6 gRNA lentiviral vector in RVLM

Nav1.6 gRNA lentiviral vector and nontargeted lentiviral vector (2.1×10^{6} TU of purified vector) was microinjected to RVLM of the SIHR on the fifth day of stress [19]. Western

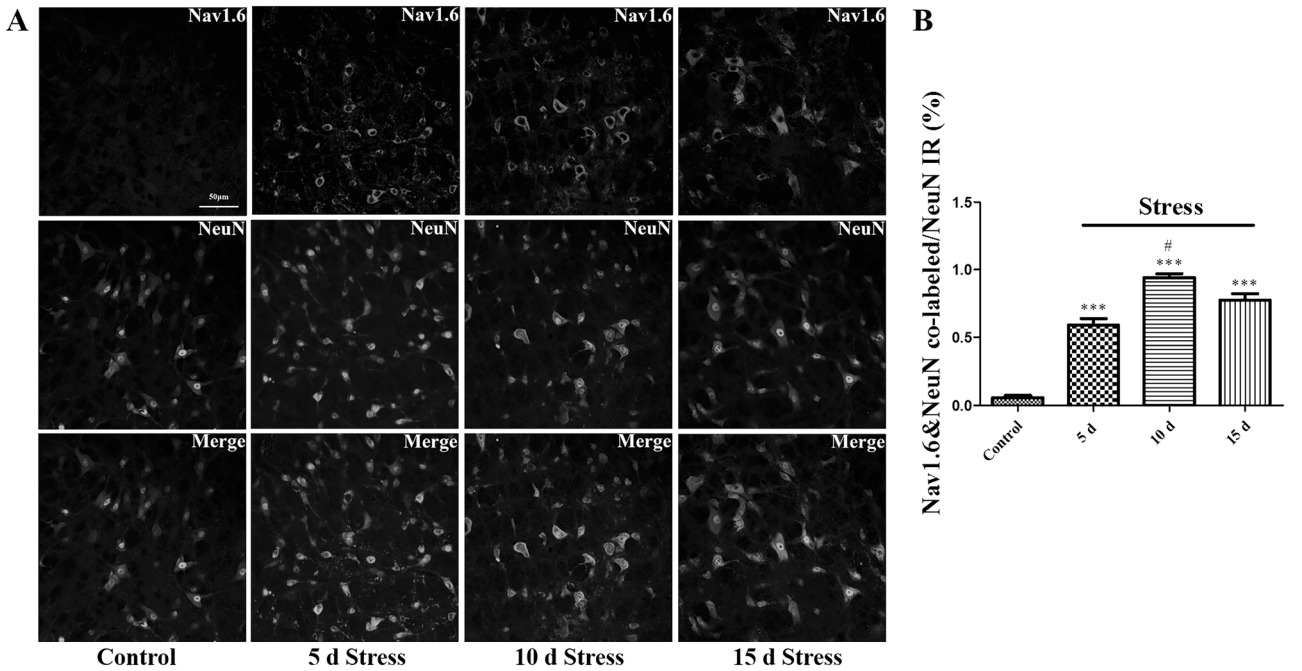

Fig. 4 Changes of Nav1.6-ir cells colocalized with NeuN in the rostral ventrolateral medulla (RVLM) of rats during consecutive days of stress. **a** Colocalization of Nav1.6 (red) with NeuN (green) in the RVLM at different time points after stress in stress-induced hypertensive rat (SIHR) and normotensive (control) group. **b** Quantitative analysis of numbers of Nav1.6-immunoreactive (ir) cells colocalized with NeuN. Note a remarkable increase in Nav1.6-ir cells within the RVLM on the 5th, 10th, and 15th day after stress, $^{***}P < 0.001$. The rate of colocalization of Nav1.6-ir with NeuN is higher on the tenth day after stress than at other time points, $^{\#}P < 0.05$, $n = 4$. Bars represent mean ± standard error

blotting was performed to investigate Nav1.6 expression at protein level in control group, SIHR, Stress + Lv-CRISPR-eGFP group and Stress + Lv-CRISPR-gRNA group. Compared with stress group, there was discernible difference in Nav1.6 protein level of the SIHR, Stress + Lv-CRISPR-eGFP group and Stress + Lv-CRISPR-gRNA group. However, Nav1.6 protein levels of Stress + Lv-CRISPR-gRNA group were significantly decreased than the SIHR and Stress + Lv-CRISPR-eGFP group, but still higher than the control group (Fig. 6a, b).

Level of SBP, HR, and RSNA began to significantly increase after 10 days of daily stress induction (Fig. 7a−c). The microinjection of Lv-CRISPR-eGFP to RVLM of the SIHR did not affect the level of SBP and RSNA compared with the stress group. The level of SBP, HR, and RSNA was significantly decreased in the Stress + Lv-CRISPR-gRNA group by microinjection of Lv-CRISPR-gRNA than the SIHR and Stress + Lv-CRISPR-eGFP group, but still higher than the control group (Fig. 7a−c).

Discussion

In this study, protein expression of the VGSC subtype Nav1.6 was significantly increased in the RVLM of the SIHR group, reaching its highest level at the tenth day of stress. Moreover, the majority of Nav1.6-ir was located in neurons rather than astrocytes or microglia. Furthermore, SBP levels and numbers of Nav1.6-ir cells were dynamically altered with continued daily induction of stress. A remarkable increase in Nav1.6 expression was observed on the tenth day of stress, the same time SBP reaches its highest level. The level of RSNA was significantly increased after 10 days of stress induction than the control group. Compared with the SIHR, knockdown of Nav1.6 in RVLM of the SIHR decreased the level of SBP, HR, and RSNA. Our results demonstrate that Nav1.6 expression in RVLM neurons contributes to the development of SIH, a feature that has not been previously reported.

Previous studies have reported that stress is a state of physical and mental tension that occurs because of various unexpected demanding factors and/or circumstances [2]. Stress causes depression with increasing SBP and sympathetic activity, which leads to increased appetite for food intake, resulting in the increased body weight [20, 21]. In previous studies, we used a stressor apparatus consisting of electric foot-shocks combined with noise, which resulted in elevated SBP and HR associated with SIH [12, 22, 23]. Activation of sympathetic neural pathways plays a key role in mediating cardiovascular diseases such as acute and chronic SIH [19, 22, 23]. The RVLM is the major location for maintenance of sympathetic vasomotor activity by

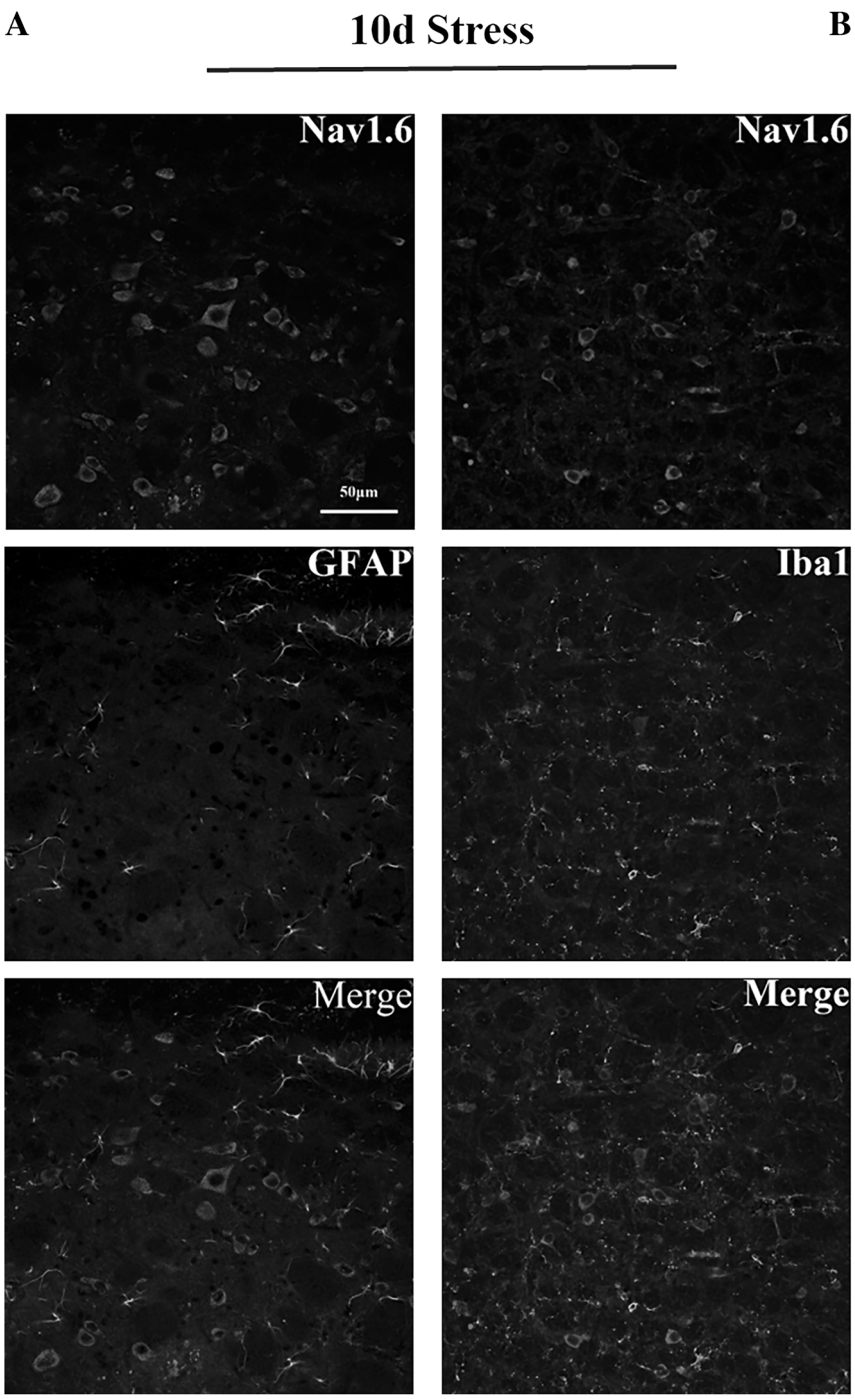

Fig. 5 Colocalization of Nav1.6 (red) with Iba1 (green) and GFAP (green) in the rostral ventrolateral medulla (RVLM) of normotensive (control) rats and stress-induced hypertensive rat (SIHR) group at the tenth day of stress. **a**, **b** Nav1.6 is seldom coexpressed with the microglia marker Iba1 or astrocyte marker GFAP

premotor neurons [24]. Increased sympathetic tone from RVLM outflow to the peripheral vasculature contributes to neural mechanisms of hypertension [25].

Baroreflex suppression is the key factor to induce a series of physiological changes, and repetitive psychogenic stress, obesity, or high sodium intake can lead to increased sympathetic activity [26]. Evidences from various studies suggested that the slowing down of HR was due to the inhibitory effect of baroreflex when blood pressure rises. Baroreflex dysfunction is an important and common characteristic of arterial hypertension, closely related to sympathetic hyperactivity and activation of tissue and plasma renin-angiotensin systems [27–29]. Therefore, we think that baroreflex should be worsened in SIH.

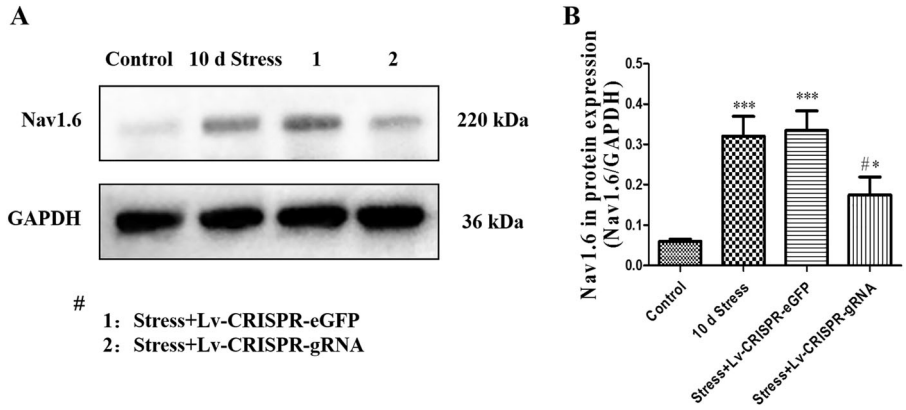

Fig. 6 Western blot analysis of Nav1.6 expression in the rostral ventrolateral medulla (RVLM) of different group. **a**, **b** Optical band density analysis revealed that Nav1.6 protein levels increased significantly at stress-induced hypertensive rat (SIHR) group at the tenth day of stress, Stress + Lv-CRISPR-eGFP group and Stress + Lv-CRISPR-gRNA group. However, the expression levels of Nav1.6 channel were significantly reduced in the Stress + Lv-CRISPR-gRNA group compared with the SIHR group at the tenth day of stress and the Stress + Lv-CRISPR-eGFP group. Bars represent mean ± standard error. $^{***}P < 0.001$, $^{*}P < 0.05$, vs. control group, $^{\#}P < 0.05$, vs. SIHR group and Stress + Lv-CRISPR-eGFP group, $n = 3$

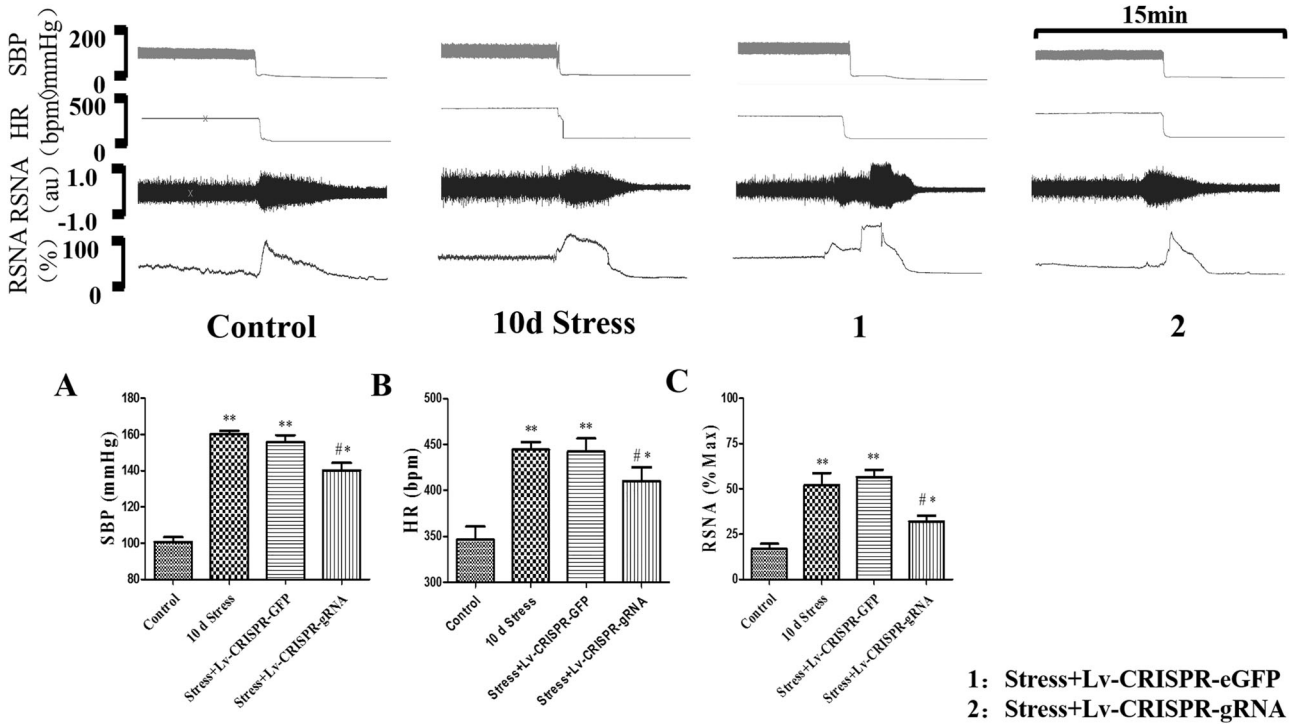

Fig. 7 Cardiovascular changes in the Stress + Lv-CRISPR-gRNA group with control group, the stress-induced hypertensive rat (SIHR) group at the tenth day of stress and the Stress + Lv-CRISPR-eGFP group. **a**–**c** Representative original tracings of SBP, HR, and RSNA in four groups. Maximum and background noise levels of RSNA were measured after rats were euthanized. The level of SBP, HR, and RSNA was remarkably decreased in the Stress + Lv-CRISPR-gRNA group compared with the SIHR group at the tenth day of stress and the Stress + Lv-CRISPR-eGFP group, but still higher than the control group. $^{**}P < 0.01$, vs. control group, $^{\#}P < 0.05$, vs. SIHR group at the tenth day of stress and the Stress + Lv-CRISPR-eGFP group, $n = 3$. Bars represent mean ± standard error

Prior investigations have demonstrated the importance of VGSCs for controlling the spread of action potentials and neuronal excitability. Increased expression of Nav1.6 results in the polarization of neuronal membrane potential, which induces overactivation of neurotransmitters (such as glutamate) and synaptic transmission [7, 8, 30]. Nav1.6 plays a key role in determining neuronal excitability within the nervous system; neuronal network hyperexcitability and spontaneous epileptiform activity arise from nervous system dysfunction in epilepsy [11]. Our present

study shows low levels of Nav1.6 expression in RVLM neurons in the control group rats and high expression in the SIHR group. In addition, an important role of Nav1.6 has been reported in sympathetic sprouting and sensory nerve activation [31]. Thus, excessive sympathetic activation by increased Nav1.6 expression in RVLM neurons may contribute to the development of SIH, as a result of nervous system dysfunction.

In addition, Nav1.6 is considered to be an important VGSC for its role in transferring action potentials, as neurons express Nav1.6. However, the limitation of prior studies is that the relationship between excessive Nav1.6 activation and SIH was not investigated. Previous reports suggest that the opening of VGSCs in response to increased intracellular Na^+ levels can increase the volume of Ca^{2+} because the Na^+/Ca^{2+} exchanger operates in reverse [32]. Excess import of Na^+ leads to neuronal activation, while increased Ca^{2+} induces a cascade of reactions that can damage and/or induce necrosis of nerve cells [33]. Our prior study demonstrated that neuronal damage or necrosis results in inflammation, which induced microglia dysfunction. Functionally degenerative microglia are unable to remove damaged neurons, resulting in sympathetic overactivity in SIH [19].

Dampney et al. have demonstrated that baroreceptor afferent fibers terminate within the nucleus tractus solitarius (NTS) and excite second-order neurons via a glutamatergic synapse. The sympathoexcitatory neurons in RVLM are activated by receiving baroreceptor signals from NTS. Sympathetic-adrenal medulla system is activated and the level of RSNA increases. The changes of RSNA from kidney project back to the RVLM and initiate a vicious circle [2, 24]. Our present study shows decreased levels of SBP and RSNA by knocking down the Nav1.6 in RVLM in the SIHR group. Thus, Nav1.6 may act as a key factor regulating neuronal hyperexcitability in the RVLM and contribute to the development of SIH.

Conclusion

The present study shows that Nav1.6 expression at protein level was significantly increased in RVLM neurons after stress induction compared to the control group; a dynamic, prominent increase of Nav1.6 immunoreactivity in neurons was observed in RVLM of SIHR. Furthermore, the upregulation of Nav1.6 expressed in RVLM neurons was strongly correlated with the SBP after stress induction. Furthermore, compared with the control group, the level of SBP and RSNA was decreased by knocking down the Nav1.6 in RVLM in the SIHR group. These findings suggest that Nav1.6 expression in RVLM neurons may contribute to the development of SIH. Further investigation will be performed to clarify the role of Nav1.6 expressed in different kind of neurons in RVLM in response to SIH.

Acknowledgements The present study was supported by the Chinese National Natural Science Foundation (grant nos. 31871151, 31571171, and 31100838), the Key Laboratory of Medical Electrophysiology (Southwest Medical University) of Ministry of Education of China (grant no. 201502) and the Young Teachers of Shanghai Universities Training Program.

Compliance with ethical standards

Conflict of interest The authors declare that they have no conflict of interest.

References

1. Lv Q, Yang Q, Cui Y, Yang J, Wu G, Liu M. et al. Effects of taurine on ACE, ACE2 and HSP70 expression of hypothalamic−pituitary−adrenal axis in stress-induced hypertensive rats. Adv Exp Med Biol. 2017;975:871–86.
2. Hering D, Lachowska K, Schlaich M. Role of the sympathetic nervous system in stress-mediated cardiovascular disease. Curr Hypertens Rep. 2015;17(10):80.
3. Dombrowski MD, Mueller PJ. Sedentary conditions and enhanced responses to GABA in the RVLM: role of the contralateral RVLM. Am J Physiol Regul, Integr Comp Physiol. 2017;313(2): R158–68.
4. Li P, Sun HJ, Cui BP, Zhou YB, Han Y. Angiotensin-(1-7) in the rostral ventrolateral medulla modulates enhanced cardiac sympathetic afferent reflex and sympathetic activation in renovascular hypertensive rats. Hypertension. 2013;61(4):820–7.
5. Dampney RA. Functional organization of central pathways regulating the cardiovascular system. Physiol Rev. 1994;74(2): 323–64.
6. Abbott SB, Stornetta RL, Socolovsky CS, West GH, Guyenet PG. Photostimulation of channelrhodopsin-2 expressing ventrolateral medullary neurons increases sympathetic nerve activity and blood pressure in rats. J Physiol. 2009;587(Pt 23): 5613–31.
7. Catterall WA, Goldin AL, Waxman SG. International Union of Pharmacology. XLVII. Nomenclature and structure−function relationships of voltage-gated sodium channels. Pharmacol Rev. 2005;57(4):397–409.
8. Catterall WA, Perez-Reyes E, Snutch TP, Striessnig J. International Union of Pharmacology. XLVIII. Nomenclature and structure−function relationships of voltage-gated calcium channels. Pharmacol Rev. 2005;57(4):411–25.
9. Zhu H, Zhao Y, Wu H, Jiang N, Wang Z, Lin W. et al. Remarkable alterations ofNav1.6 in reactive astrogliosis during epileptogenesis. Sci Rep. 2016;6:38108
10. Chen Y, Yu FH, Sharp EM, Beacham D, Scheuer T, Catterall WA. Functional properties and differential neuromodulation of Na(v)1.6 channels. Mol Cell Neurosci. 2008;38(4):607–15.
11. Hargus NJ, Nigam A, Bertram EH 3rd, Patel MK. Evidence for a role of Nav1.6 in facilitating increases in neuronal hyperexcitability during epileptogenesis. J Neurophysiol. 2013;110(5): 1144–57.
12. Xia CM, Shao CH, Xin L, Wang YR, Ding CN, Wang J. et al. Effects of melatonin on blood pressure in stress-induced hypertension in rats. Clin Exp Pharmacol & Physiol. 2008;35(10): 1258–64.

13. Hao F, Gu Y, Tan X, Deng Y, Wu ZT, Xu MJ. et al. Estrogen replacement reduces oxidative stress in the rostral ventrolateral medulla of ovariectomized rats. Oxid Med Cell Longev. 2016;2016:2158971
14. Platt RJ, Chen S, Zhou Y, Yim MJ, Swiech L, Kempton HR. et al. CRISPR-Cas9 knockin mice for genome editing and cancer modeling. Cell . 2014;159(2):440–55.
15. Lorincz A, Nusser Z. Molecular identity of dendritic voltage-gated sodium channels. Science. 2010;328(5980):906–9.
16. Paxinos G. The rat nervous system. Oxford: Elsevier Academic Press; 2004.
17. Zhu H, Lin W, Zhao Y, Wang Z, Lao W, Kuang P. et al. Transient upregulation of Nav1.6 expression in the genu of corpus callosum following middle cerebral artery occlusion in the rats. Brain Res Bull. 2017;132:20–27.
18. Hu W, Tian C, Li T, Yang M, Hou H, Shu Y. Distinct contributions of Na(v)1.6 and Na(v)1.2 in action potential initiation and backpropagation. Nat Neurosci. 2009;12(8): 996–1002.
19. Du D, Hu L, Wu J, Wu Q, Cheng W, Guo Y. et al. Neuroinflammation contributes to autophagy flux blockage in the neurons of rostral ventrolateral medulla in stress-induced hypertension rats. J Neuroinflamm. 2017;14(1):169
20. Michopoulos V, Toufexis D, Wilson ME. Social stress interacts with diet history to promote emotional feeding in females. Psychoneuroendocrinology. 2012;37(9):1479–90.
21. Shi S, Liang J, Liu T, Yuan X, Ruan B, Sun L. et al. Depression increases sympathetic activity and exacerbates myocardial remodeling after myocardial infarction: evidence from an animal experiment. PLoS ONE. 2014;9(7):e101734
22. Xiao F, Jiang M, Du D, Xia C, Wang J, Cao Y. et al. Orexin A regulates cardiovascular responses in stress-induced hypertensive rats. Neuropharmacology. 2013;67:16–24.
23. Zhang CR, Xia CM, Jiang MY, Zhu MX, Zhu JM, Du DS. et al. Repeated electroacupuncture attenuating of apelin expression and function in the rostral ventrolateral medulla in stress-induced hypertensive rats. Brain Res Bull. 2013; 97:53–62.
24. Dampney RA, Coleman MJ, Fontes MA, Hirooka Y, Horiuchi J, Li YW. et al. Central mechanisms underlying short- and long-term regulation of the cardiovascular system. Clin Exp Pharmacol & Physiol. 2002;29(4):261–8.
25. Guyenet PG. The sympathetic control of blood pressure. Nat Rev Neurosci. 2006;7(5):335–46.
26. Raffai G, Cseko C, Nadasy G, Kocsis L, Dézsi L, Hunyor SN. et al. Environmental stress and vestibular inputs modulate cardiovascular responses to orthostasis in hypertensive rats. Hypertens Res. 2018;41(1):18–26.
27. La Rovere MT, Bersano C, Gnemmi M, Specchia G, Schwartz PJ. Exercise-induced increase in baroreflex sensitivity predicts improved prognosis after myocardial infarction. Circulation. 2002; 106(8):945–9.
28. Cohuet G, Struijker-Boudier H. Mechanisms of target organ damage caused by hypertension: therapeutic potential. Pharmacol Ther. 2006;111(1):81–98.
29. Iliescu R, Tudorancea I, Irwin ED, Lohmeier TE. Chronic baroreflex activation restores spontaneous baroreflex control and variability of heart rate in obesity-induced hypertension. Am J Physiol Heart Circ Physiol. 2013;305(7):H1080–1088.
30. Goldberg EM, Coulter DA. Mechanisms of epileptogenesis: a convergence on neural circuit dysfunction. Nat Rev Neurosci. 2013;14(5):337–49.
31. Xie W, Strong JA, Zhang JM. Local knockdown of the NaV1.6 sodium channel reduces pain behaviors, sensory neuron excitability, and sympathetic sprouting in rat models of neuropathic pain. Neuroscience. 2015;291:317–30.
32. Kirischuk S, Kettenmann H, Verkhratsky A. Na+/Ca2+exchanger modulates kainate-triggered Ca2+signaling in Bergmann glial cells in situ. FASEB J. 1997;11(7):566–72.
33. Lange I, Moschny J, Tamanyan K, Khutsishvili M, Atha D, Borris RP. et al. Scrophularia orientalis extract induces calcium signaling and apoptosis in neuroblastoma cells. Int J Oncol. 2016;48(4):1608–16.